Section 2. Relaxation theory and data treatment

Anomalous diffusion and relaxation in macromolecular systems

A. Blumen [a,*], A.A. Gurtovenko [a,b], S. Jespersen [a,c]

[a] *Theoretische Polymerphysik, Universität Freiburg, Hermann-Herder-Str. 3, D-79104 Freiburg, Germany*
[b] *Institute of Macromolecular Compounds, Russian Academy of Sciences, Bolshoi Prospect 31, V.O., St. Petersburg 199004, Russia*
[c] *Institute of Physics and Astronomy, University of Aarhus, DK-8000 Århus C, Denmark*

Abstract

Scaling, namely the algebraic (power-law) dependence of measured properties on frequency or time is of wide-spread occurrence in polymeric systems. In this work we highlight its connection to fractional calculus. As examples of systems that obey scaling, we discuss here linear and fractal generalized Gaussian structures. On the other hand, non-scaling behavior is also found in many realistic situations. In the second part of the paper we consider as example of non-scaling behavior the relaxation of small-world networks. Detailed measurements, such as provided by dielectric spectroscopy or mechanical relaxation can help to determine the basic, mesoscopic properties of the substances under investigation. © 2002 Elsevier Science B.V. All rights reserved.

1. Introduction

Regular diffusion, better known as Brownian motion, is characterized (in the absence of directed, external fields) by a linear increase of the mean-square displacement with time. For anomalous diffusion, a feature of common occurrence in polymeric systems, as we will recall in the following, this simple relation does not hold; the temporal evolution of the mean-square displacement is non-linear and often obeys at long times

$$\overline{\mathbf{R}^2(t)} \sim t^{\gamma} \tag{1}$$

with $\gamma \neq 1$. In the case $\gamma < 1$ one denotes the behavior as subdiffusive. For simply structured particles (the ideal case being point-like objects) such a pattern of motion often results from disorder [1–5]; for polymeric materials – which may be envisaged as being built out of beads (monomers) connected by springs – the motion of the monomers also obeys Eq. (1) in the absence of disorder; the reason for this is due to the relaxation of the internal modes of the structure [6]. Furthermore, Eq. (1) is also obeyed during several motional stages in melts of polymer chains; then one has reptation [7], and the processes giving rise to disentanglement are characterized by different exponents γ in Eq. (1) [7–9]. In the case $\gamma > 1$ the motion

---

[*] Corresponding author. Fax: +49-761 203 5906.
  E-mail address: blumen@physik.uni-freiburg.de (A. Blumen).

is termed superdiffusive. Classical examples for superdiffusive behavior are furnished by the motion of particles in turbulent flows [4,10] and by the motion of polymers in layered flows [11].

In recent times, besides the classical way of describing anomalous diffusion via continuous time random walks (CTRW) and Lévy-walks models [1–4,10,12–16], also descriptions based on fractional derivatives have attracted much interest [17,18]. In this article we will stress the fact, by following the developments outlined in Refs. [19,20], that anomalous diffusion in the scaling form of Eq. (1) is closely connected to heuristic descriptions based on fractional derivatives. As we proceed to show, such relations are particularly useful because they allow to invert in a simple way the integral expressions which follow from the theory of linear response. Such transformations, however, do not hold when the anomaly does not have a power-law character.

In order to show that such non-power-law (non-scaling) behaviors can readily appear in more complex, network-type situations, we focus on small-world networks (SWN), and analyse their response to external fields. In so doing we keep in mind that most measurements are performed in the frequency-domain; we exemplify our findings with expressions typical for mechanical relaxation and for dielectric spectroscopy.

Before turning to specific examples we note that in many instances, such as in the presence of a constant, non-zero electric field (say, oriented along the y-axis), Eq. (1) turns out to be equivalent [8,20,21] to the relation

$$\overline{Y(t)} \sim t^\gamma, \tag{2}$$

where we have $\boldsymbol{R} = (X, Y, Z)$.

2. Fractional derivatives and their connection to anomalous dynamics

In order to model the viscoelastic properties of polymers one may start by combining a spring and a dashpot sequentially. Denoting by σ the stress and by ε the strain one has for the spring

$$\sigma_1(t) = E\varepsilon_1(t) \tag{3}$$

and for the dashpot

$$\sigma_2(t) = \eta \frac{\mathrm{d}\varepsilon_2(t)}{\mathrm{d}t}, \tag{4}$$

where E is related to Young's modulus and η to the viscosity. The sequential arrangement of spring and dashpot is the so-called Maxwell model [22], whose constitutive equation reads

$$\sigma + \tau \frac{\mathrm{d}\sigma}{\mathrm{d}t} = \tau E \frac{\mathrm{d}\varepsilon}{\mathrm{d}t} \tag{5}$$

with $\tau = \eta/E$. The response of $\sigma(t)$ to a stepwise change in $\varepsilon(t)$, i.e. to $\varepsilon(t) = \varepsilon_0\theta(t)$ is called the relaxation modulus $G(t)$. For the Maxwell model one has from Eq. (5), see also Ref. [22],

$$G(t) = E\varepsilon_0\mathrm{e}^{-t/\tau}. \tag{6}$$

Relaxation measurements are often performed in the frequency, ω-domain, and not in the time-domain. Exemplarily, one often measures the storage modulus

$$G'(\omega) \equiv \omega \int_0^\infty G(t)\sin(\omega t)\,\mathrm{d}t \tag{7}$$

and the loss modulus

$$G''(\omega) \equiv \omega \int_0^\infty G(t)\cos(\omega t)\,\mathrm{d}t, \tag{8}$$

which in the case of the Maxwell model read

$$G'(\omega) = \frac{(\omega\tau)^2}{(\omega\tau)^2 + 1}E\varepsilon_0 \tag{9}$$

and

$$G''(\omega) = \frac{\omega\tau}{(\omega\tau)^2 + 1}E\varepsilon_0. \tag{10}$$

Unfortunately, detailed measurements show that many polymers do not obey such forms [19,20]. The behavior of many classes of polymers is much better described by changing the derivatives in the constitutive equation, Eq. (5) to fractional derivatives. As a reminder, one has as defining relation for fractional derivation the Riemann–Liouville expression

$$\frac{\mathrm{d}^\alpha f}{\mathrm{d}t^\alpha} \equiv \frac{1}{\Gamma(-\alpha)} \int_0^t \frac{f(\tilde{t})}{(t-\tilde{t})^{\alpha+1}}\,\mathrm{d}\tilde{t}. \tag{11}$$

$\Gamma(z)$ in Eq. (11) is the Gamma-function, and the expression extends the (integer) recursive integra-

tion to the domain of real α; differentiation is obeyed for $\alpha > 0$, integration for $\alpha < 0$. Since we focus on polymers we are in the case of subdiffusive motion, see Section 1, so that α in Eq. (11) is bounded, $0 < \alpha < 1$. For technical reasons and because of an intimate relation to linear response we prefer to extend in Eq. (11) the lower integration limit to $-\infty$; in this way we obtain the Weyl-form of fractional calculus [23]. For the Weyl-calculus in general the differentiation rule

$$\frac{d^\alpha f}{dt^\alpha} = \frac{d^\beta}{dt^\beta}\left(\frac{d^{\alpha-\beta}f}{dt^{\alpha-\beta}}\right) \qquad (12)$$

holds, when one restricts conveniently the set of functions f [23]. Now it turns out that replacing the usual derivatives by Weyl-fractional derivatives in the constitutive equation of the Maxwell-model, Eq. (5), leads to

$$\sigma(t) + \tau^{\alpha-\beta}\frac{d^{\alpha-\beta}\sigma(t)}{dt^{\alpha-\beta}} = \tau^\alpha E\frac{d^\alpha \varepsilon(t)}{dt^\alpha} \quad (\text{with } \alpha > \beta). \qquad (13)$$

Distinct from Eq. (5) it turns out that Eq. (13) offers an excellent description for many polymeric substances, see Refs. [19,20] for details. As we proceed to show, the underlying reason for the success of Eq. (13) is the fact that it is intimately related to the scaling of the kernel of the response function; scaling, however, is wide-spread in polymer physics.

We follow here the description of Ref. [20] in order to show that the Weyl-form of fractional calculus mirrors in a powerful mathematical way the behavior of materials whose internal processes obey algebraic decays. Denoting by $\Phi(t)$ the response of the system to an external perturbation $\Psi(t)$, one can express the relation between these two functions in terms of $\Phi_s(t)$, the response of the system to a step perturbation $\theta(t)$ of Ψ. In the framework of linear response one has, because of the superposition principle and of causality,

$$\Phi(t) = \int_{-\infty}^{t} d\tilde{t}\,\Phi_s(t-\tilde{t})\frac{d\Psi(\tilde{t})}{d\tilde{t}}. \qquad (14)$$

In general Eq. (14) is difficult to invert, being an integral relation. However, for Φ_s algebraic, i.e.

$\Phi_s \equiv [C/\Gamma(1-\alpha)](\tau_0/t)^\alpha$, where $0 < \alpha < 1$, it follows that

$$\Phi(t) = C\tau_0^\alpha\frac{1}{\Gamma(1-\alpha)}\int_{-\infty}^{t}\frac{d\tilde{t}}{(t-\tilde{t})^\alpha}\frac{d\Psi(\tilde{t})}{d\tilde{t}}$$
$$= C\tau_0^\alpha\frac{d^\alpha\Psi(t)}{dt^\alpha}, \qquad (15)$$

where we used the repeated differentiation as given in Eq. (12). Clearly now, Eq. (15) can be readily inverted, since it is a simple fractional derivative. The inversion reads

$$\Psi(t) = \frac{1}{C\tau_0^\alpha}\frac{d^{-\alpha}\Phi(t)}{dt^{-\alpha}}. \qquad (16)$$

Evidently, one can simply read-off from Eq. (16), by inverting the argument leading from Eq. (14) to Eq. (15), that the response $\Psi_s(t)$ to a step perturbation $\theta(t)$ of Φ is

$$\Psi_s(t) = \frac{C^{-1}}{\Gamma(1+\alpha)}\left(\frac{t}{\tau_0}\right)^\alpha \quad \text{for } t > 0. \qquad (17)$$

Alternatively, one can also verify that $\Psi_s(t)$ corresponds indeed to $\Phi(t) = \theta(t)$ by inserting $\Psi_s(t)$ into the integral of Eq. (15). The integral turns then for $t > 0$ into the Beta function $B(1-\alpha,\alpha) = \Gamma(1-\alpha)\Gamma(\alpha)$, see Eqs. 3.191(3) and 8.384 of Ref. [24], from which $\Phi(t) = \theta(t)$ follows.

Eq. (17) makes clear that now the strain (extension) of the object under an external stress (force) obeys, due to $0 < \alpha < 1$, just the subdiffusive law expressed by Eq. (2). Given now that many macromolecular systems show such subdiffusive behaviors [7–9,20], it becomes evident why they can be described very well using expressions involving fractional derivatives; as long as the response is linear, scaling behavior and fractional description are just two sides of the same coin.

3. Generalized Gaussian structures and scaling

To focus our ideas on a particular type of model we now perform our study in the framework of the Rouse model [8,25] and of its extension to generalized Gaussian structures (GGS) [26–28]. A GGS consists of beads subject to friction (with friction constant ζ) connected to each other by springs (with elasticity constant K). In the Langevin framework,

the position vector $r_l(t)$ of the lth bead of the GGS, subject to the external force $F_l(t)$, obeys

$$\zeta \frac{\mathrm{d}r_l(t)}{\mathrm{d}t} + K \sum_{m=1}^{N} A_{lm} r_m(t) = F_l(t) + \zeta w_l(t), \qquad (18)$$

where $\mathbf{A} = \{A_{lm}\}$ is the connectivity matrix of the GGS (see Refs. [26–28] for details), $\zeta w_l(t)$ is the thermal noise (here assumed to be Gaussian, with zero mean-value), and N is the total number of elements (beads) in the system considered. The linear system of difference-differential equations given by Eq. (18) can be completely solved through the diagonalization of the matrix $\mathbf{A}$, see e.g. Ref. [28], a procedure which involves in general determining both the eigenvalues and the eigenfunctions of $\mathbf{A}$. For simplicity, we focus only on the stretching (extension) of the GGS under a constant external force $F(t) = F\theta(t)e_y$, switched on at $t = 0$ and acting only on a single bead, say the lth, in the y-direction. As discussed in Refs. [28,29], the displacement of the bead along the y-direction, $Y(t)$, reads after averaging both over the fluctuating forces $w_l(t)$ and over all the beads of the GGS

$$\overline{Y(t)} = \frac{F}{\zeta N} t + \frac{F\tau_0}{\zeta} \frac{1}{N} \sum_{i=2}^{N} \frac{1 - \exp(-\lambda_i(t/\tau_0))}{\lambda_i}, \qquad (19)$$

where $\tau_0 = \zeta/K$. This expression is very simple, it involves *only* the eigenvalues λ_i (but not the eigenvectors) of the connectivity matrix $\mathbf{A}$. One may note that in Eq. (19) the motion of the center of mass has separated automatically from the rest. Clearly, the behavior of the motion for extremely short and for very long times is obvious: One has in the limit of very short times, from Eq. (19), $\overline{Y(t)} \sim Ft/\zeta$, whereas for very long times one attains $\overline{Y(t)} \sim Ft/(N\zeta)$. This is a very general feature, which makes clear that the particular structure of the GGS under investigation (and thus information about its structural matrix $\mathbf{A}$) is revealed only in the intermediate time domain. This is also the domain which may show anomalous dynamics.

Now in the case of a Gaussian chain, when the force acts on one end of the chain, the displacement $\overline{Y_0(t)}$ simplifies to [8,20]

$$\overline{Y_0(t)} = \frac{F}{N\zeta} t + \frac{2F}{N\zeta} \sum_{p=1}^{\infty} \int_0^t \mathrm{d}\tau \exp(-p^2\tau/\tau_{\mathrm{R}}), \qquad (20)$$

where τ_{R} denotes the Rouse-time

$$\tau_{\mathrm{R}} = \frac{\zeta N^2}{\pi^2 K}, \qquad (21)$$

which is the longest internal relaxation time of the Rouse chain [8,25]. A simple calculation shows that at short and medium times one obtains as dominant contribution for the displacement (averaged over all beads)

$$\overline{Y(t)} \sim \frac{F}{\sqrt{\zeta K}} t^{1/2} \quad \text{for } t \ll \tau_{\mathrm{R}}, \qquad (22)$$

which indeed scales according to Eq. (2) with $\gamma = 1/2$. Another scaling relation is obeyed when the generalized Gaussian structure is not a simple chain, but a regular fractal. In this case one obtains, under the same conditions

$$\overline{Y(t)} \sim \frac{F}{\zeta^{1-d_s/2} K^{d_s/2}} t^{1-d_s/2} \quad \text{for } d_s < 2, \qquad (23)$$

as long as d_s, the so-called spectral dimension, is less than two. Again this relation corresponds to Eq. (2), with $\gamma = 1 - d_s/2$.

4. Non-scaling behavior: measurable expressions

In this section we will highlight experiments which allow one to show that for many GGS, scaling – as given by Eq. (2) – does not hold. Several topological structures do not obey scaling, the most prominent of which are hyper-branched polymers and, as a special case, dendrimers [21,28,30]. In this paper we center on SWN [31–36]. In so doing we will focus on readily measurable quantities for such systems; these are, apart from the above discussed displacement $\overline{Y(t)}$, Eq. (19), also mechanical and dielectric relaxation forms. The mechanical side is exemplified by the complex dynamic modulus $G^*(\omega)$ or, equivalently, by its real $G'(\omega)$ and imaginary $G''(\omega)$ components, given for $\omega > 0$ by (see also Eqs. 4.159 and 4.160 of Ref. [8])

$$G'(\omega) = v k_B T \frac{1}{N} \sum_{i=2}^{N} \frac{(\omega \tau_0 / 2\lambda_i)^2}{1 + (\omega \tau_0 / 2\lambda_i)^2} \qquad (24)$$

and

$$G''(\omega) = v k_B T \frac{1}{N} \sum_{i=2}^{N} \frac{\omega \tau_0 / 2\lambda_i}{1 + (\omega \tau_0 / 2\lambda_i)^2}, \qquad (25)$$

where v is the number of polymer segments (beads) per unit volume, λ_i are the eigenvalues of the connectivity matrix $\mathbf{A}$ of the system, and $\tau_0 = \zeta/K$. The $\lambda_1 = 0$ mode corresponds to the translation of the whole GGS and may influence in $G''(\omega)$ only in the very close vicinity of $\omega = 0$. Note that the factor 2 in the relaxation times $\tau_i = \tau_0/2\lambda_i$ arises from the second moment of the displacements involved in computing the stress needed in the evaluation of $G^*(\omega)$ [8]. As discussed before in a special case, Eqs. (9) and (10), the quantities $G'(\omega)$ and $G''(\omega)$ are the storage and the loss modulus, respectively [22,37].

The dielectric relaxation forms are based on the frequency-dependent complex dielectric susceptibility $\varepsilon^*(\omega)$. As shown recently, dielectric relaxation is very revealing of complex media, such as percolation structures and fractals [38,39]. As a special model which leads to convenient, simple forms we focus here on the dielectric response of GGSs, which possess dipole moments directed along their bonds (type A in the usual nomenclature) [40–42]. One has generally for the $\varepsilon^*(\omega)$ of polar molecules embedded in non-polar solvents under an alternating electric field $E = E_0 \exp(i\omega t)$ [43]:

$$\Delta\varepsilon^*(\omega) = \frac{\varepsilon^*(\omega) - \varepsilon_\infty}{\varepsilon_0 - \varepsilon_\infty} \simeq \int_0^\infty \left(-\frac{\mathrm{d}}{\mathrm{d}t} C_0(\mathbf{M}; t) \right)$$
$$\times \exp(-i\omega t)\,\mathrm{d}t. \qquad (26)$$

In this equation any local fields are ignored. The ε_0 and ε_∞ denote the limiting low- and high-frequency dielectric constants, respectively, and $C_0(\mathbf{M}; t)$ is the normalized autocorrelation function of the total dipole moment $\mathbf{M}(t)$ of the system, $C_0(\mathbf{M}; t) = \langle \mathbf{M}(0)\mathbf{M}(t) \rangle / \langle \mathbf{M}^2(0) \rangle$. Now, in our A-type model we assign a longitudinal dipole moment $\mathbf{m}_j$ to each bond j of the GGS; we consider in the following the special case that the magnitude of each $\mathbf{m}_j$ is directly proportional to

the length of the jth bond, but that the orientation of the $\{\mathbf{m}_j\}$ along the bonds is random and uncorrelated. It is then a straightforward matter to show that also for general GGS (and not only for linear chains [8]) $C_0(\mathbf{M}; t)$ averaged over all possible orientation distributions is a simple sum involving the GGS bonds only [44], since

$$\langle \mathbf{M}(0)\mathbf{M}(t) \rangle = \mu^2 \sum_{j=1}^{N_b} \langle \mathbf{u}_j(0)\mathbf{u}_j(t) \rangle. \qquad (27)$$

Here the index j goes over all the N_b, bonds of the GGS, μ is the absolute value of the dipole moment per unit length, and $\mathbf{u}_j = \mathbf{r}_l - \mathbf{r}_m$ is the vector of the jth bond between the lth and the mth GGS bead. The approach presented here parallels that developed for the dielectric relaxation of regular mesh-like networks built from macromolecules with longitudinal dipole moments [45] as well as that for the mechanical relaxation of a regular lattice decorated with subunits [46]. Putting these results together, it follows that

$$C_0(\mathbf{M}; t) = \frac{1}{N} \sum_{i=1}^{N} \exp(-\lambda_i t / \tau_0), \qquad (28)$$

where, as before, the λ_i are the eigenvalues of the GGS connectivity matrix $\mathbf{A}$ and N is the total number of beads in the GGS. The reason why $C_0(\mathbf{M}; t)$ takes the simple form, Eq. (28), is due to the fact that the potential energy U of the GGS, which enters in the Langevin equation, Eq. (18), equals [26,27]

$$U = \frac{K}{2} \sum_{j=1}^{N_b} \mathbf{u}_j^2 = \frac{K}{2} \sum_{l,m=1}^{N} A_{lm}\mathbf{r}_l\mathbf{r}_m. \qquad (29)$$

Therefore, the transformation which diagonalizes $\mathbf{A}$, automatically reduces $\langle \mathbf{M}(0)\mathbf{M}(t) \rangle$, Eq. (27), to a sum of exponents, from which Eq. (28) follows.

Inserting now Eq. (28) in Eq. (26) leads immediately to the following expressions for the real and the imaginary parts of the dielectric susceptibility $\Delta\varepsilon^* = \Delta\varepsilon' - \mathrm{i}\Delta\varepsilon''$:

$$\Delta\varepsilon'(\omega) = \frac{1}{N} \sum_{i=2}^{N} \frac{1}{1 + (\omega \tau_0 / \lambda_i)^2} \qquad (30)$$

and

$$\Delta\varepsilon''(\omega) = \frac{1}{N}\sum_{i=2}^{N}\frac{\omega\tau_0/\lambda_i}{1+(\omega\tau_0/\lambda_i)^2}. \qquad (31)$$

It should be noted in particular that the dielectric susceptibility $\Delta\varepsilon^*(\omega)$, Eqs. (30) and (31), is determined by relaxation times which are twice larger than those appearing in the expressions of mechanical relaxation, Eqs. (24) and (25). As already stressed, for calculating $G^*(\omega)$ as well as $\Delta\varepsilon^*(\omega)$ we need only the eigenvalues λ_i (or the corresponding relaxation times τ_i) of the small-world Rouse network (SWRN), but not the eigenfunctions.

5. Small-world Rouse networks: numerical calculations

In this section we focus on GGS based on SWNs, the so-called SWRN; recently such SWRNs were used to model disordered cross-linked polymers [29] by employing the GGS-extension of the Rouse model [26–28,47–49]. Such SWRNs are of great theoretical interest, since they interpolate between linear Rouse chains and disordered polymer networks.

One very interesting property of SWNs consists in the appearance of a so-called 'pseudogap' in the density of states [34], namely, a fairly large spacing between the minimal non-vanishing eigenvalue and the zero eigenvalue of the SWN under study. It is thus of importance to see how this theoretical concept and also the general non-scaling behavior of the density of states translate into observable quantities, such as $\overline{Y(t)}$, the averaged bead-motion in external fields, the mechanical $G'(\omega)$ and $G''(\omega)$ moduli, and the dielectric $\varepsilon'(\omega)$ and $\varepsilon''(\omega)$ relaxation forms. Exemplarily, we studied $\overline{Y(t)}$ for SWRN and have shown that it does not obey Eq. (2); a much better description is provided e.g. by the form $\overline{Y(t)} \sim (Ft/N\zeta) - C't^{1/6}\exp(-C''t^{1/3})$ with C' and C'' constants [29]. In the following we center on the SWRN-expressions related to $G^*(\omega)$ and to $\varepsilon^*(\omega)$.

We follow here the SWRN construction of Ref. [29], with the exception that we start from a linear Rouse chain, and not from a ring; the initial chain consists of N beads, connected by elastic springs [8,25]. Then we add additional links (AL), i.e.

springs, by connecting each bead of the chain with probability q/N to another bead, picked randomly. In this way beads distant from each other along the macromolecular backbone may (due to the AL) get to be close in space.

We begin by evaluating $G'(\omega)$ and $G''(\omega)$, Eqs. (24) and (25). In order to obtain λ_i, the corresponding eigenvalues, we proceed as follows: starting from specific realisations of SWRNs, for $N = 1000$, we determine the corresponding connectivity matrices $\mathbf{A}$, Eq. (18). Using standard routines for the diagonalization of symmetric matrices [50], we obtain the N eigenvalues λ_j of each matrix $\mathbf{A}$. In order to ascertain how the differences in SWRN realisations influence the results, we compare these for 10 distinct SWRN realisations. In Figs. 1 and 2 we plot in double logarithmic scales the reduced (dimensionless) storage $G'(\omega)/vk_BT$ and loss $G''(\omega)/vk_BT$ moduli as a function of the reduced frequency $\omega\tau_0$; for $q = 0.05$, $q = 0.1$, and $q = 0.5$ we present the two extremal results (from 10). We infer that the differences are rather small and that the shapes of the curves are very similar. Note that the differences decrease with increasing q, indicating that results for SWRNs with small q are most prone to differ from realisation to realisation. This may be under-
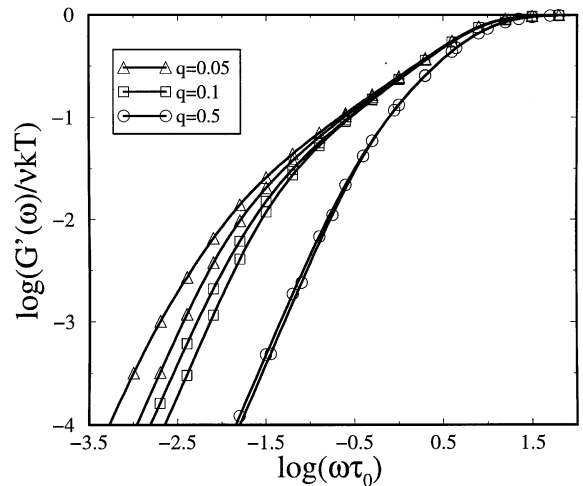
Fig. 1. The reduced storage modulus $G'(\omega)/vk_BT$ plotted in double logarithmic scales vs the reduced frequency $\omega\tau_0$. Shown are results for the two extreme realisations (from 10) for SWRN with $N = 1000$ and $q = 0.05$ ($\triangle$), $q = 0.1$ ($\square$), and $q = 0.5$ ($\bigcirc$).
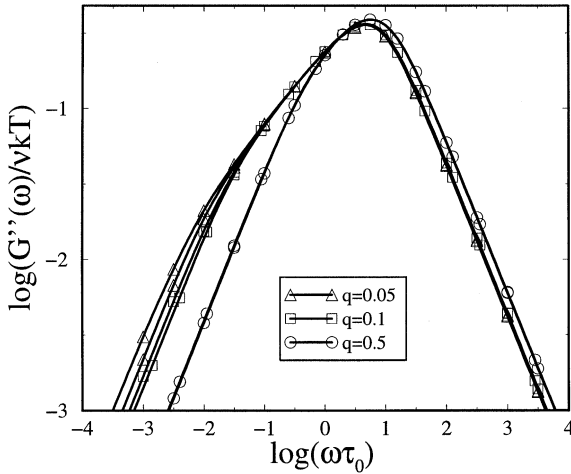
Fig. 2. The reduced loss modulus $G''(\omega)/vk_BT$ plotted in double logarithmic scales vs the reduced frequency $\omega\tau_0$. Shown are results for the two extreme realisations (from 10) for SWRN with $N = 1000$ and $q = 0.05$ ($\triangle$), $q = 0.1$ ($\square$), and $q = 0.5$ ($\bigcirc$).
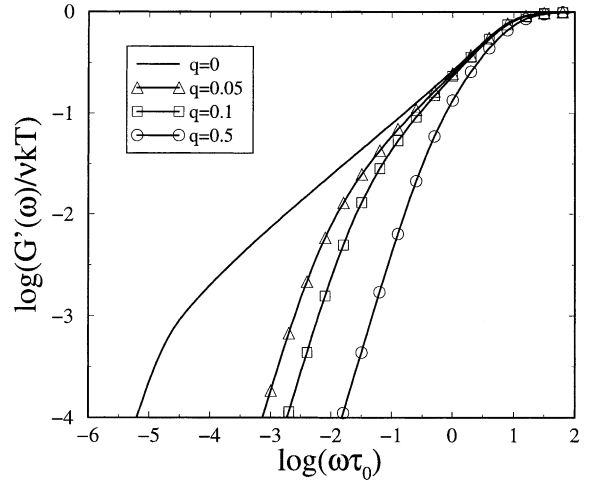
Fig. 3. The reduced storage modulus $G'(\omega)/vk_BT$ plotted in double logarithmic scales vs the reduced frequency $\omega\tau_0$. Shown are results for the SWRN with $N = 1000$ and $q = 0$ (—), $q = 0.05$ ($\triangle$), $q = 0.1$ ($\square$), and $q = 0.5$ ($\bigcirc$). The averaging is performed over 100 realisations of the SWRN.

stood from the fact that for fixed q the distribution in the number N_{AL} of AL is binomial; then $\langle N_{AL}\rangle = Nq$, $\langle N_{AL}^2\rangle - \langle N_{AL}\rangle^2 = Nq(1-q)$ and $(\langle N_{AL}^2\rangle - \langle N_{AL}\rangle^2)/\langle N_{AL}\rangle^2 = (1-q)/Nq$ is a measure for the relative fluctuations; note that it gets big for small q. Moreover, Figs. 1 and 2 indicate that $G'(\omega)$ is more sensitive to the structural details than $G''(\omega)$. Thus for $q = 0.5$ the curves for $G''(\omega)$ are practically indistinguishable, whereas changes in $G'(\omega)$ are still discernible.

In Figs. 3 and 4 we plot for $N = 1000$ the SWRN $G'(\omega)$ and $G''(\omega)$, averaged over 100 different realisations. In order to display the dependence of $G'(\omega)$ and $G''(\omega)$ on q, we let it take the values 0, 0.05, 0.1, and 0.5. The case $q = 0$ is the standard Rouse chain, whose $G'(\omega)$ and $G''(\omega)$ are well known [8]. From Fig. 3 one can distinguish very clearly, for $q = 0$, three characteristic scaling domains for $G'(\omega)$; these scale (from low frequencies ω) as ω^2, $\omega^{1/2}$, and ω^0, respectively. $G'(\omega)$ in the low-frequency domain, which in Fig. 3 corresponds to $\omega\tau_0 < 10^{-5}$, is given by the small-$\omega\tau_0$ expansion of Eq. (24), and goes as ω^2; in the high-frequency domain, in Fig. 3 given by $\omega\tau_0 > 1$, $G'(\omega)$ tends towards a constant, as evident from Eq. (24). The non-trivial behavior is the intermediate one; for the Rouse chain, $q = 0$, one finds a
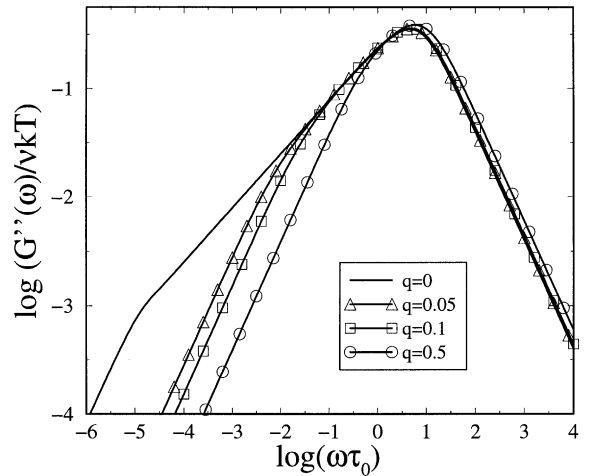
Fig. 4. The reduced loss modulus $G''(\omega)/vk_BT$ plotted in double logarithmic scales vs the reduced frequency $\omega\tau_0$. Shown are results for the SWRN with $N = 1000$ and $q = 0$ (—), $q = 0.05$ ($\triangle$), $q = 0.1$ ($\square$), and $q = 0.5$ ($\bigcirc$). The averaging is performed over 100 realisations of the SWRN.

$\omega^{1/2}$-law for over four orders of magnitude in ω, see Fig. 3. This behavior changes drastically when $q \neq 0$, as is evident from Fig. 3; even a small amount of ALs destroys scaling in the intermediate range. Moreover, the intermediate range itself

gets to be smaller; this is due to the fact that the ALs lead to the disappearance of low-lying modes in the SWRN (the pseudogap situation). Hence by starting from $q = 0$ and increasing q, the ω^2-curves of Fig. 3 shift dramatically to the right. This fact can be used to experimentally determine changes in the spectrum due to the ALs.

A similar conclusion can be drawn for $G''(\omega)$. Now $G''(\omega)$ displays a maximum, see Fig. 4. The position of the maximum is mainly determined by the rather high frequency modes, which correspond to the motion of just a few SWRN beads; hence this position depends only weakly on q. All curves in Fig. 4 show a similar behavior for small and for large ω. Expanding Eq. (25) for small and for large ω one obtains readily that for very small ω one has $G''(\omega) \sim \omega$, whereas for very large ω one has $G''(\omega) \sim \omega^{-1}$. Of particular interest is the intermediate behavior, which for a Rouse chain ($q = 0$) shows the usual scaling behavior $G''(\omega) \sim \omega^{1/2}$, which is clearly evident in Fig. 4 on the left side of the maximum. Even a slight increase of q immediately wipes out this intermediate scaling behavior. Clearly, as found before in the case of $G'(\omega)$, the algebraic scaling is extremely sensitive to even a few ALs which get superimposed on the linear chain and transform it into a SWRN. Also clearly evident from Fig. 4 is the fact that the largest deviations from the $q = 0$ curve happen on the low-energy-side, again reflecting the fact that it is here that most changes of the spectrum occur; this is the region corresponding to the pseudogap, connected to a cut-off in the internal SWRN relaxation modes and to a shift in the appearance of the so-called terminal relaxation for very small ω. The reason why in the high-frequency domain the changes in $G'(\omega)$ and $G''(\omega)$ (Figs. 3 and 4) are rather small in going from $q = 0$ to $q = 0.5$ is physically clear; in the high-frequency domain one sees the local dynamics, which involves only a few beads, and which is hence little affected by the ALs.

Another interesting feature in Fig. 4 is the fact that the maximum of $G''(\omega)$ gets higher with increasing q. Recalling that $G''(\omega)$ accounts for the loss of energy in the system, which is due, on the microscopic scale, to the friction of the beads in the viscous medium, it is clear that all SWRNs

with the same number of beads N have the same energy loss, regardless of q. Now the total loss of energy, E_{loss}, is proportional to [8,42]

$$
\begin{aligned}
E_{\text{loss}} &\sim \int_0^\infty \sum_{i=2}^N \frac{\tau_0/2\lambda_i}{1 + (\omega\tau_0/2\lambda_i)^2}\, \mathrm{d}\omega \\
&= \sum_{i=2}^N \int_0^\infty \frac{\omega\tau_0/2\lambda_i}{1 + (\omega\tau_0/2\lambda_i)^2}\, \mathrm{d}\ln\omega.
\end{aligned}
\tag{32}
$$

Since each of the integrals on the right-hand-side of Eq. (32) is equal to $\pi/2$, the total sum is $(N-1)\pi/2$ (an additional $\pi/2$ term comes from $\lambda_1 = 0$, see the remarks after Eq. (25)). Hence the total surface under the curve $G''(\omega)$, plotted (distinct from Fig. 4) semi-logarithmically with respect to ω, should be the same for all q values. Given that with increasing q the loss modulus $G''(\omega)$ gets to be strongly changed (squeezed) in the low-frequency domain and that $G''(\omega)$ is only very weakly dependent on q in the high-frequency domain, it follows that the maximal value of $G''(\omega)$ increases with q. Our reasoning is clearly confirmed by Fig. 4, which shows an increase of the maximum of $G''(\omega)$ with q.

The numerical evaluation of the components $\Delta\varepsilon'(\omega)$ and $\Delta\varepsilon''(\omega)$ of the dielectric susceptibility $\Delta\varepsilon^*(\omega)$ of SWRNs proceeds analogously to the evaluation of the components of $G^*(\omega)$. In fact, only $\Delta\varepsilon'(\omega)$ needs to be computed, since from Eqs. (25) and (31) $G''(\omega)$ and $\Delta\varepsilon''(\omega)$ are (apart from the factor of 2 multiplying the λ_i) proportional to each other. Hence the dielectric loss factor $\Delta\varepsilon''(\omega)$ has practically the same frequency dependence as the loss modulus $G''(\omega)$; the only difference being the fact that the relaxation times of $\Delta\varepsilon''(\omega)$ are twice as large as those of $G''(\omega)$. Hence, due to the logarithmic scales of Fig. 4, the plot of $\Delta\varepsilon''(\omega)$ differs from the corresponding plot of the reduced $G''(\omega)/vk_BT$ only by a shift along the ω-axis. Turning now to $\Delta\varepsilon'(\omega)$, we evaluate it for SWRNs with $N = 1000$, averaged over 100 realisations, where q is equal to 0, 0.05, 0.1, and 0.5, respectively. The plots are given in Fig. 5, again, in double logarithmic scale. At low frequencies, $\omega\tau_0 \ll 1$, for the Rouse chain, i.e. $q = 0$, $\Delta\varepsilon'(\omega)$ obeys $|\Delta\varepsilon'(\omega) - 1| \sim (\omega\tau_0)^2$, i.e. it deviates only slightly from a constant. At larger frequencies, one
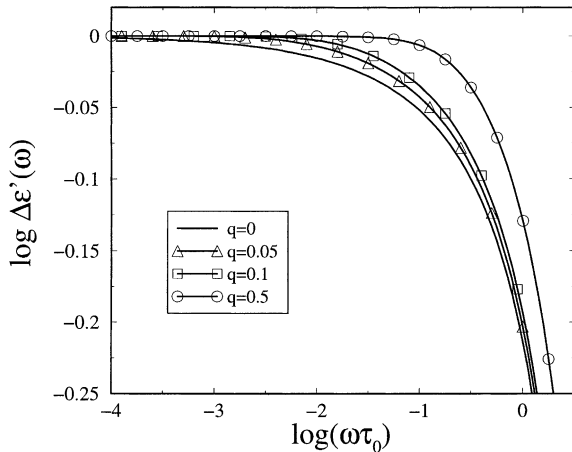
Fig. 5. The real part of the dielectric susceptibility $\Delta\varepsilon'(\omega)$ plotted in double logarithmic scales vs the reduced frequency $\omega\tau_0$. Shown are results for the SWRN with $N = 1000$ and $q = 0$ (—), $q = 0.05$ ($\triangle$), $q = 0.1$ ($\square$), and $q = 0.5$ ($\bigcirc$). The averaging is performed over 100 realisations of the SWRN.

observes for $q = 0$ first a domain dominated by the internal Rouse-relaxation of the chain, in which $|\Delta\varepsilon'(\omega) - 1| \sim (\omega\tau_0)^{1/2}$, followed, at high frequencies, $\omega\tau_0 > 1$, by the usual Debye decay, $\Delta\varepsilon'(\omega) \sim (\omega\tau_0)^{-2}$. As before, by increasing q (i.e. increasing the ALs) the smallest eigenvalues (maximum relaxation times) of the SWRN increase (decrease). Thus in Fig. 5 the frequency domain corresponding to the internal SWRN relaxation becomes shorter and sets in at higher frequencies; this can be visualized as an increase in the rigidity of the SWRNs with increasing q. On the high-frequency side, with increasing q, the curves tend to become steeper, see Fig. 5.

Summarizing, both the mechanical and the dielectrical relaxation properties of SWRNs depend in their intermediate ω-domain strongly on the number of ALs inserted into the linear chain. We infer that SWRNs belonging to different values of q can be readily distinguished, through judicious experiments.

6. Conclusions

Anomalous diffusion, often characterized by a power-law dependence of the mean-square displacement of a moving particle on time, arises in a number of different physical situations. Such scaling often shows up in other measurable quantities, such as mechanical response and dielectric relaxation functions. Here we stressed how a description in terms of fractional calculus can be very convenient when dealing with scaling systems, e.g. by using fractional kinetic equations to describe the power-law response of such systems to external perturbations. As examples of systems that display power-law dynamics, we discussed linear and fractal generalized Gaussian structures. However, many systems behave in more complicated ways and thus their response deviates from simple scaling. Here we treated in detail one class of such systems, namely the so-called SWRNs. We focused on four measurable quantities: the storage modulus, the loss modulus, and the real and imaginary parts of the dielectric susceptibility. From general analytical expressions involving only the eigenvalues of the associated connectivity matrix, we evaluated numerically these quantities. The results display a wide variety of non-scaling behaviors and depend strongly on the number of additional links inserted into the regular Rouse chain. We were able to explain the shape of the ensuing curves by invoking the increased rigidity of the SWRN with increasing q, a fact related to the pseudogap concept.

References

[1] H. Scher, M. Lax, Phys. Rev. B 7 (1973) 4491, 4502.
[2] H. Scher, E.W. Montroll, Phys. Rev. B 12 (1975) 2455.
[3] M.F. Shlesinger, J. Stat. Phys. 36 (1984) 639.
[4] G. Zumofen, A. Blumen, J. Klafter, M.F. Shlesinger, J. Stat. Phys. 54 (1989) 1519.
[5] H. Schiessel, G. Oshanin, A. Blumen, J. Chem. Phys. 103 (1995) 5070.
[6] A. Blumen, Philos. Mag. B 81 (2001) 1021.
[7] P.-G. de Gennes, Scaling Concepts in Polymer Physics, Cornell University, Ithaca, NY, 1979.

[8] M. Doi, S.F. Edwards, The Theory of Polymer Dynamics, Clarendon, Oxford, 1986.

[9] A.Yu. Grosberg, A.R. Khokhlov, Statistical Physics of Macromolecules, AIP, New York, 1994.

[10] J. Klafter, A. Blumen, M.F. Shlesinger, Phys. Rev. A 35 (1987) 3081.

[11] S. Jespersen, G. Oshanin, A. Blumen, Phys. Rev. E 63 (2001) 011801.

[12] E.W. Montroll, G.H. Weiss, J. Math. Phys. 6 (1965) 167.

[13] A. Blumen, J. Klafter, B.S. White, G. Zumofen, Phys. Rev. Lett. 53 (1984) 1301.

[14] H. Schnörer, D. Haarer, A. Blumen, Phys. Rev. B 38 (1988) 8097.

[15] A. Blumen, G. Zumofen, J. Klafter, Phys. Rev. A 40 (1989) 3964.

[16] A. Blumen, H. Schnörer, Angew. Chem. 102 (1990) 158; Angew. Chem. Int. Ed. 29 (1990) 113.

[17] R. Hilfer (Ed.), Applications of Fractional Calculus in Physics, World Scientific, Singapore, 2000.

[18] R. Metzler, J. Klafter, Phys. Rep. 339 (2000) 1.

[19] C. Friedrich, H. Schiessel, A. Blumen, in: D.A. Siginer, D. DeKee, R.P. Chhabra (Eds.), Advances in the Flow and Rheology of Non-Newtonian Fluids, Elsevier, Amsterdam, 1999, p. 429.

[20] H. Schiessel, C. Friedrich, A. Blumen, in: R. Hilfer (Ed.), Applications of Fractional Calculus in Physics, World Scientific, Singapore, 2000, p. 331.

[21] P. Biswas, R. Kant, A. Blumen, J. Chem. Phys. 114 (2001) 2430.

[22] I.M. Ward, Mechanical Properties of Solid Polymers, 2nd Ed., J. Wiley, Chichester, 1985.

[23] K.B. Oldham, J. Spanier, The Fractal Calculus, Academic Press, New York, 1974.

[24] I.S. Gradshteyn, I.M. Ryzhik, Table of Integrals, Series, and Products, 4th Ed., Academic Press, New York, 1965.

[25] P.E. Rouse, J. Chem. Phys. 21 (1953) 1272.

[26] J.-U. Sommer, A. Blumen, J. Phys. A 28 (1995) 6669.

[27] H. Schiessel, Phys. Rev. E 57 (1998) 5775.

[28] P. Biswas, R. Kant, A. Blumen, Macromol. Theory Simul. 9 (2000) 56.

[29] S. Jespersen, I.M. Sokolov, A. Blumen, J. Chem. Phys. 113 (2000) 7652.

[30] R. Kant, P. Biswas, A. Blumen, Macromol. Theory Simul. 9 (2000) 608.

[31] D.J. Watts, S.H. Strogatz, Nature (London) 393 (1998) 440.

[32] M.E.J. Newman, D.J. Watts, Phys. Rev. E 60 (1999) 7332.

[33] M. Barthélémy, L.A.N. Amaral, Phys. Rev. Lett. 82 (1999) 3180.

[34] R. Monasson, Eur. Phys. J. B 12 (1999) 555.

[35] M.E.J. Newman, C. Moore, D.J. Watts, Phys. Rev. Lett. 84 (2000) 3201.

[36] S. Jespersen, I.M. Sokolov, A. Blumen, Phys. Rev. E 62 (2000) 4405.

[37] J.D. Ferry, Viscoelastic Properties of Polymers, 3rd Ed., J. Wiley, New York, 1980.

[38] Y. Feldman, R. Nigmatullin, E. Polygalov, J. Texter, Phys. Rev. E 58 (1998) 7561.

[39] T. Saraidarov, E. Axelrod, Y. Feldman, R. Reisfeld, Chem. Phys. Lett. 324 (2000) 7.

[40] W.H. Stockmayer, M.E. Baur, J. Am. Chem. Soc. 86 (1964) 3485.

[41] W.H. Stockmayer, Pure Appl. Chem. 15 (1967) 539.

[42] H. Yamakawa, Modern Theory of Polymer Solutions, Harper and Row, New York, 1971.

[43] G. Williams, Chem. Rev. 72 (1972) 55.

[44] A.A. Gurtovenko, A. Blumen, Macromolecules 35 (2002) 3288.

[45] Yu.Ya. Gotlib, A.A. Gurtovenko, Macromol. Theory Simul. 5 (1996) 969.

[46] A.A. Gurtovenko, A. Blumen, J. Chem. Phys. 115 (2001) 4924.

[47] B.E. Eichinger, J.E. Martin, J. Chem. Phys. 69 (1978) 4595.

[48] A. Kloczkowski, J.E. Mark, H.L. Frisch, Macromolecules 23 (1990) 3481.

[49] M. Guenza, A. Perico, Macromolecules 25 (1992) 5942.

[50] W.H. Press, B.P. Flannery, S.A. Teukolsky, W.T. Vetterling, Numerical Recipes in C. The Art of Scientific Computing, Cambridge University, New York, 1988.